Finite element analysis of the light distribution of the near infrared probe to assist brain neurosurgical guidance

Lijuan Dai (戴丽娟), Zhiyu Qian (钱志余), and Huinan Wang (王惠南)

Department of Biomedical Engineering, Nanjing University of Aeronautics and Astronautics, Nanjing 210016

Finite element analysis is used to study the near infrared light distribution in brain tissue. The diameter of the light beam varies from 100 μm to 1 mm. The researching results indicate that the near infrared light distribution in brain tissue gets wider with rising of the beam diameter, and the distribution fields are 0.05–0.2 mm below the probe, respectively. At last, the results of finite element analysis are verified by Monte-Carlo simulation, which prove the feasibility of using near infrared light in brain surgical guidance.

OCIS codes: 290.1990, 290.7050, 300.6340.

Recently, the near infrared (NIR) spectrum technique has widely applications in biomedical field[1,2]. The study of optical image reconstruction[3] has made the NIR image available as a real time surgery guidance, which will be very useful in brain surgery for the brain tissues' displacements or distortions induced by dehydration, export of the cerebrospinal fluid, or the ablation of the soft tissue during the surgical process[4,5]. In this paper, the NIR light distribution is discussed by finite element analysis (FEA) to prove the feasibility of the NIR image guidance in brain surgery. Monte-Carlo simulation is used to verify the results of FEA, which is a new method in tissue optical research.

In tissue optics, diffusion theory has been applied widely[6]. When tissue's absorption coefficient is far less than its reduced scattering coefficient and its anisotropy factor is equal to 1, the diffusion transmitting equation can be simplified into[7]

$$\frac{1}{c}\frac{\partial}{\partial t}\Phi(r,t) - D\nabla^2\Phi(r,t) + \mu_{\rm a}\Phi(r,t) = S(r,t), \qquad (1)$$

where $\Phi(r,t)$ is the light flux in the r distance to the light source; t is the responsive time; c is the velocity of the light transmitting in the tissue; $S(r,t)$ is the light source power; $\mu_{\rm a}$ is the tissue's absorption coefficient; and diffusion coefficient D has the following expression:

$$D = \frac{1}{3[\mu_{\rm a} + (1-g)\mu_{\rm s}]} = \frac{1}{3(\mu_{\rm a} + \mu_{\rm s}')}, \qquad (2)$$

where $\mu_{\rm s}$, $\mu_{\rm s}'$, g are tissue's scattering coefficient, reduced scattering coefficient, and anisotropy factor, respectively.

Table 1 is a list of some values of brain tissue's optical properties digested from Ref. [8], which shows that brain tissue's $\mu_{\rm a}$ is far less than its $\mu_{\rm s}'$ and its g is almost equal to 1, so the light transmitting status in brain tissue can be known by solving Eq. (1). For the simulation requirement can only be a coarse range, the simulation data of $\mu_{\rm a}$, $\mu_{\rm s}'$ in this paper are estimated from Table 1. The $\mu_{\rm s}'$ estimated is 4–40 cm^{-1}, and the $\mu_{\rm a}$ is 0.1–0.3 cm^{-1}. FEMLAB is chosen to solve the Eq. (1). FEMLAB has been applied widely in physics, mechanics, and images processing, etc., however, there are few reports concerned about its applications in tissue optics.

Above all, for the penetration depth is far less than the tissue's thickness, the tissue can be regarded as a kind of mean medium. Firstly, a 4×4 (cm) square representing the brain tissue is drawn in FEMLAB. The diameter of the light beam is varied from 100 μm to 1 mm, and the light intensity is 1 J. The probe's position is set 10 μm to the tissue's inferior surface. Simulations are done to three different brain tissues whose optical parameters are shown in Table 2. Figures 1–4 are some results digested from the simulations.

Light distribution in brain white matter at different source diameter is described by Fig. 1. It can be seen that the distribution region get wider as the diameter of the light beam rising, but as the scattering coefficient of brain white matter is relatively great, the distribution region in this medium is small, for instance, 0.15 cm below the probe for 400-μm light source. The similar distribution law shares in the brain gray matter and the general brain matter, whereas they all have bigger distribution regions than the brain white matter. Their differences are obviously shown in Fig. 2 where compares the light intensity along the tissue depth in the three different tissues for 400-μm light source. It can be seen in Fig. 2 that the distribution regions are respectively 0.2 and 0.3 cm below the probe in the general brain matter and the brain gray matter.

Secondly, the effects of $\mu_{\rm a}$ and $\mu_{\rm s}'$ are studied. The size of the brain tissue is same with the above in FEMLAB. The diameter of the light beam is 400 μm and the light intensity is 1 J. First $\mu_{\rm a}$ is fixed to 0.1 cm^{-1}, simulations are done when $\mu_{\rm s}'$ is orderly selected as 4, 10, 15, 20, 25, 30, 35, 40 cm^{-1} to study the distribution regions at different $\mu_{\rm s}'$. Then, $\mu_{\rm s}'$ is fixed to 20 cm^{-1}, simulations are done when $\mu_{\rm a}$ is orderly selected as 0.1, 0.2, 0.3 cm^{-1} to study the distribution regions at different $\mu_{\rm a}$.

The changes of the light intensity along the depth are represented in Fig. 3 when the tissue's $\mu_{\rm a}$ is fixed and

Table 1. Some Optical Properties of Brain Tissue[8]

Type	Method	$\mu_{\rm a}$ (cm^{-1})	$\mu_{\rm s}'$ (cm^{-1})	g
Adult Brain White Matter	*In Vitro*	3.2 ± 0.4	60 ± 3	0.87
Adult Brain Gray Matter	*In Vitro*	2.7 ± 0.4	20 ± 2	0.94
Child Brain White Matter	*In vivo*	0.13	9.8	—
Child Brain Gray Matter	*In vivo*	0.19	4.8–7.4	—

Table 2. Simulation Data of Brain White Matter, Gray Matter, and General Brain Tissue

Type	μ_s' (cm^{-1})	μ_a (cm^{-1})	D (cm)
Brain White Matter	40	0.1	0.0083
Brain Gray Matter	4	0.3	0.078
General Brain Tissue	10	0.15	0.033

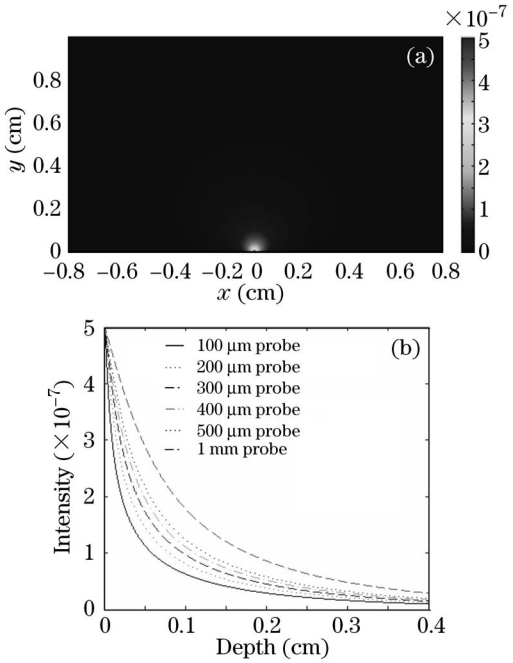

Fig. 1. Light distribution in brain white matter at different probe sources. (a) 2D map of light distribution in brain white matter at 100-μm probe beam, (b) light intensity versus depth at different probes in brain white matter ($\mu_s' = 40$ cm^{-1}, $\mu_a = 0.1$ cm^{-1}).

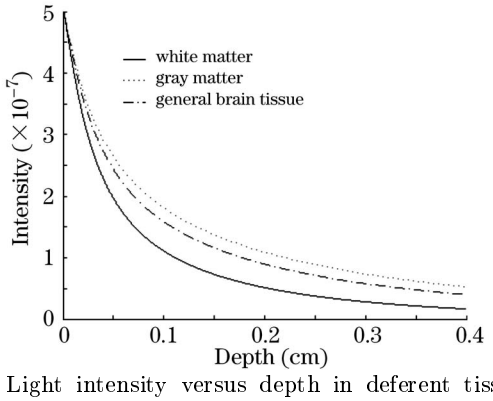

Fig. 2. Light intensity versus depth in deferent tissues at 400-μm probe source.

its μ_s' is orderly changed, from which a conclusion can be made that the light distribution region gets smaller as the scattering coefficient rises, but along with the accretion, its effect to the light distribution region gets weaker. When μ_s' is fixed, the changes of μ_a affect little to the light distribution region as it can be seen in Fig. 4.

Finally, Monte-Carlo simulation is used to verify the simulation results of FEMLAB. Monte-Carlo simulation

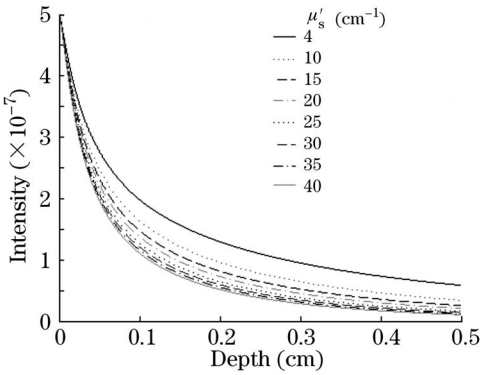

Fig. 3. Light intensity versus depth in tissues of different reduced scattering coefficients ($\mu_a = 0.1$ cm^{-1}).

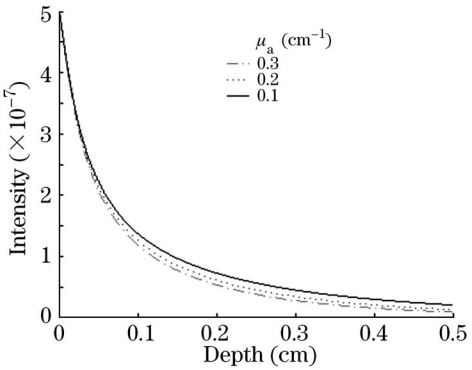

Fig. 4. Light intensity versus depth in tissues of different absorption coefficients ($\mu_s' = 20$ cm^{-1}).

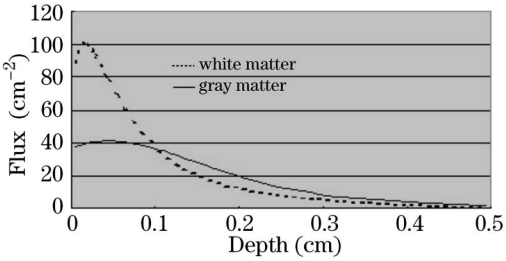

Fig. 5. Light flux versus depth in brain white matter and gray matter at 400-μm light beam by Monte-Carlo simulation.

consumes long time but its result is usually taken as a standard to verify the accuracy of other methods in tissue optics. The program of Monte-Carlo simulation used here is written by Wang[9]. The simulation results in brain white matter and gray matter are shown in Fig. 5. The diameter of the light beam is 400 μm and the light intensity is 1 J. For the different principles of the two simulation methods, the light intensity of the two simulations is different within the 0.1-cm region, especially to the brain gray matter. However, the results of the two simulations tend to be similar when light goes deeply into the tissue.

In conclusion, the light distribution results of Monte-Carlo simulation and FEMLAB are similar, which show a NIR light distribution region within 0.4 cm below the probe in brain tissue, and for the light beam used in this paper, i.e., 100 μm to 1 mm, the light distribution regions are respectively 0.05–0.2 cm below the probe, and the light distribution region in the brain gray matter is

greater than the one in the brain white matter. All these data prove the feasibility of using near infrared light in brain surgical guidance.

FEMLAB is a new method in tissue optics, which can simulate at different theoretical models and solve the diffusion theoretical equation conveniently. Its process is simple and quick and its figures are easily understandable. When the light distribution region in the tissue is only need, FEMLAB can be chosen instead of Monte Carlo simulation and its results are reliable.

This work was supported by the National Natural Science Foundation of China (No. 30371362). L. Dai's e-mail address is viviantea@tom.com.

References

1. G. Yoon, D. N. G. Roy, and R. C. Straight, Appl. Opt. **32,** 580 (1993).
2. V. C. Peters, D. R. Wyman, M. S. Patterson, and G. L. Frank, Phys. Med. Biol. **35,** 1317 (1990).
3. B. Chance, E. Anday, S. Nioka, S. Zhou, L. Hong, K. Worden, C. Li, T. Murray, Y. Ovetsky, D. Pidikiti, and R. Thomas, Opt. Express **2,** 411 (1998).
4. C. Ling, C. Z. Hui, and L. W. Jing, Medical Equipment **16,** (10) 6 (2003).
5. Z. Z. Huang, C. S. Ping, and T. D. Chun, China Medical Device Information (in Chinese) **8,** (3) 21 (2002).
6. L. J. Cheng, L. Z. Hua, and H. A. Zhi, Acta Laser Biology Sin. (in Chinese) **13,** (3) 167 (2004).
7. M. S. Patterson, B. Chance, and B. C. Wilson, Appl. Opt. **12,** 2331 (1989).
8. W. F. Cheong, S. A. Prahl, and A. J. Welch, IEEE J. Quantum Electron. **26,** 2166 (1990).
9. L. H. Wang, S. L. Jacques, and L. Q. Zheng, Computer Methods and Programs in Biomedicine **47,** 131 (1995).